# Carbonate Chemistry variability in the East coast of Gran Canaria island

Laura Vázquez Álvarez

Curso 2019/2020

Magdalena Santana-Casiano

Melchor González-Dávila

FACULTAD DE CIENCIAS DEL MAR

UNIVERSIDAD DE LAS PALMAS DE GRAN CANARIA

# Carbonate Chemistry variability in the East Coast of Gran Canaria island

**Laura Vázquez Álvarez**

Curso 2019/2020

Trabajo de fin de título presentado por LAURA VÁZQUEZ ÁLVAREZ para la obtención del título de **Grado en Ciencias del Mar** por la Universidad de las Palmas de Gran Canaria

TUTORES:

Melchor González Dávila, Instituto de Oceanografía y Cambio Global, Departamento de Química, Facultad de Ciencias del Mar, Universidad de Las Palmas de Gran Canaria

J. Magdalena Santana Casiano, Instituto de Oceanografía y Cambio Global, Departamento de Química, Facultad de Ciencias del Mar, Universidad de Las Palmas de Gran Canaria

Laura Vázquez Álvarez  Melchor González Dávila  J. Magdalena Santana Casiano

# INDEX

# 1. INTRODUCTION

## 1.1. Carbonate system variability: Marine acidification

In a natural occurring way, there have always been great variability of greenhouse gases concentration in the atmosphere (carbon dioxide, nitrous oxide, methane). Those oscillations have always presented a quite constant range over the last 650 thousand years before the Industrial Revolution. From then on, in 1750, the greenhouse gases' concentrations have suffered a sharp increase due to emissions from anthropogenic activities (*Joos and Spahni, 2007*).

A 31-years register of the variation in carbon dioxide concentration at the Izaña weather station, at Northeast of Tenerife island, can be seen in Figure 1.

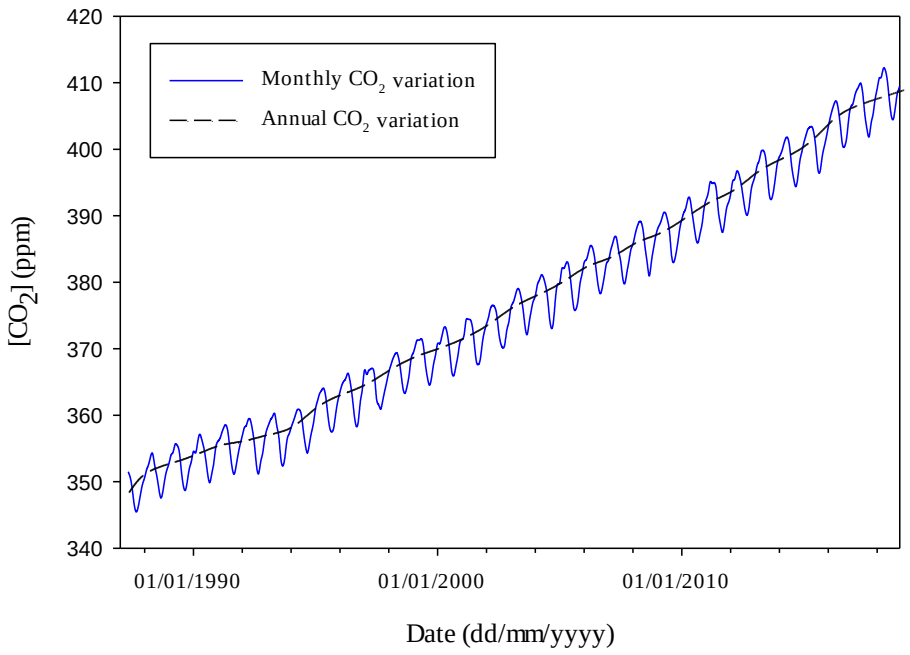


Figure 1. Atmospheric $CO_2$ concentration (in ppm), registered in the Izaña weather station (Tenerife Island), from 1987 to 2018. Source: https://www.epdata.es/asi-aumentado-concentracion-co2/2f1e490f-4a53-4534-a9c0-40f2860316bc , viewed the 17th April 2020.

Carbon dioxide has the capacity to be transferred through the atmosphere-ocean interface, been able to go in both ways, depending on relative concentrations, and other factors, such as wind speed, tidal current and bottom stress, whereas the wind speed is the most considered (*Chen et al., 2013).* When it enters the carbon cycle of seawater, it is controlled by physical, chemical and biological processes: solubility pump, biological pump and carbonate pump (*Millero, 2013*).

Depending on which ambient – air or water – is been assisted by the exchange of $CO_2$, the ocean act as source or sink of carbon dioxide. Due to the great rise of $CO_2$ in the atmosphere mentioned before, the surface of ocean acting as a sink (*Borges, 2011*) has rose in size and magnitude, giving rise to the carbon dioxide concentration in the marine environment. Since pre-industrial years, the sea has absorbed almost a third part of the gas released to the atmosphere by human activities (*Frölicher et al., 2015).*

Ocean acidification is a process by which the atmospheric $CO_2$ uptake causes an increase in its concentration in the marine environment, decreasing the pH and carbonate ions from water. To be able to understand the way in which the ocean can be altered by acidification, it is necessary to know the normal operation of the carbonate system, which is dominated by the reactions (*Millero, 2013*):

1. $CO_2 + H_2O \leftrightarrow H_2CO_3$ — $CO_2$ reacts in contact with water, creating carbonic acid.
2. $H_2CO_3 \leftrightarrow H^+ + HCO_3^-$ — Carbonic acid rapidly dissociates, giving rise to hydrogen ions and bicarbonates.
3. $HCO_3^- \leftrightarrow H^+ + CO_3^{2-}$ — Bicarbonate dissociates as well, generating mor hydrogen ions that, which in turn react back again with the carbonate ions, decreasing its concentration.

Ocean acidification process has several effects in biogeochemistry of marine environment, that can be summarized into biological and metal speciation changes. The sea surface waters decrease in pH has as predominant effects the carbonate and hydroxide ($CO_3^{2-}$ and $OH^-$) concentration reductions. The $CO_3^{2-}$ lowering in seawater produces a reduction in calcium carbonate minerals ($CaCO_3^{2-}$), such as calcite or aragonite, which makes calcifying organisms, whose shells and skeletons depend on those minerals, have difficulties for their correct formation (*Melendez and Salisbury, 2017, Millero et al. 2009*).

Metals present in marine environment form strong inorganic complexes with $CO_3^{2-}$ and $OH^-$, so their concentration decrease caused by the pH drop produces great changes in the speciation of those metals: as the concentration of the complex they are mainly linked to is reduced, their free forms are benefited, at the same time as their thermodynamic and kinetic activity increase. The rise in the concentration of free metal ions in seawater means an increase in their bioavailability that, in several cases can be toxic for some organisms, as they were adapted to quite low concentrations by efficient uptake mechanisms (*Millero et al. 2009*).

Marine acidification has also effects in some rate processes, such as redox process in metals, i.e. cupper or iron. In the cupper case, an $CO_3^{2-}$ increase develops its oxidized form, as Cu(II) tends to form complexes with carbonates. Therefore, a $CO_3^{2-}$ lowering produced by pH drop will benefit the reduced form of cupper, Cu(I). Something similar

occurs with iron: the lower pH increases its reduced form, Fe(II), that is the most soluble and bioavailable form of iron (*Hoffmann et al. 2012, Millero et al. 2009, Samperio-Ramos et al. 2016*). However, the biogeochemical effects of most of these processes remain unknown, so it is required further study about the consequences of increases in bioavailability and toxicity of metals for marine organisms.

## 1.2. Marine acidification in coastal zones.

Coastal areas account for 7% of the total ocean surface, and host between 14 and 30% of total primary production of the entire ocean (*Gattuso et al., 1998*), meaning that matter fluxes in those areas are disproportionate to their size.

These zones have a wide spatiotemporal variability due to their great ecosystem heterogeneity, so it is complicated to estimate the atmosphere-water carbon flows, coupled with the scarcity of data (*Borges et al. 2005*)Therefore, there are divergences in the estimates made, ranging from a flux of -0.22 $PgC.year^{-1}$, in *Cai et al., (2006)* study, to -1.0 $PgC.year^{-1}$, in *Tsunogai et al., (1999)* study. These estimates are made by extrapolating a flux from a given area, or several areas by collecting previous researches, so the representativeness of the chosen area to all coastal areas will mark the greatest or least adequacy to real values.

Most of the studies agree in the fact that coastal zones act as sinks of atmospheric $CO_2$ to the ocean, excluding coastal zones of high biological productivity such as stuaries, shall marshes or mangroves, that tend to release $CO_2$, acting as relatively weak sources of carbon dioxide due to their generally low wind speed rates (*Chen et al., 2013*). What researches also agree in is that the flux is highly influenced by the latitude, with high and temperate latitude coastal zones acting as sink, and subtropical and tropical latitudes acting as source of carbon dioxide, due to the biological productivity differences (*Chen et Borges, 2009*).

Coast is affected by its surrounding systems: atmosphere, land and open ocean (*Borges, 2011*). These three environments have the capacity of exchanging big quantities of energy and matter with coastal areas, altering their biogeochemistry. Human activities affect in a great way in how these systems interact:

- Land use determines the types and concentrations of wastewater discharges and agricultural fertilizers released.
- Greenhouse gases emissions released to the atmosphere define the deposition of elements in the sea surface.
- Climate changes affect to the biogeochemical and dynamical operation of open ocean, that bring these changes to the coast.

Due to these anthropogenic inputs of external nutrients, there are investigation (*Borges and Gypens 2010*; *Wallace et al., 2014*) showing that variations in carbonate chemistry in coastal zones can be greater dominated by eutrophication rather than marine acidification.

## 1.3. Place of study: Canary Islands Region

Canary Islands are located in between 28º - 31º N and 10º - 20º W, in the transitional zone between the northwest African coastal upwelling, and the open ocean oligotrophic waters of the subtropical gyre. This location gives intermediate characteristics, with high variability in time and in space (*Santana-Casiano et al., 2007*). The islands present a natural barrier to the equatorward flow of the Canary Current, and trade winds, giving birth to several meso-scale phenomena, mainly in the south part of the islands, such as eddies (*Arístegui et al., 1994*).

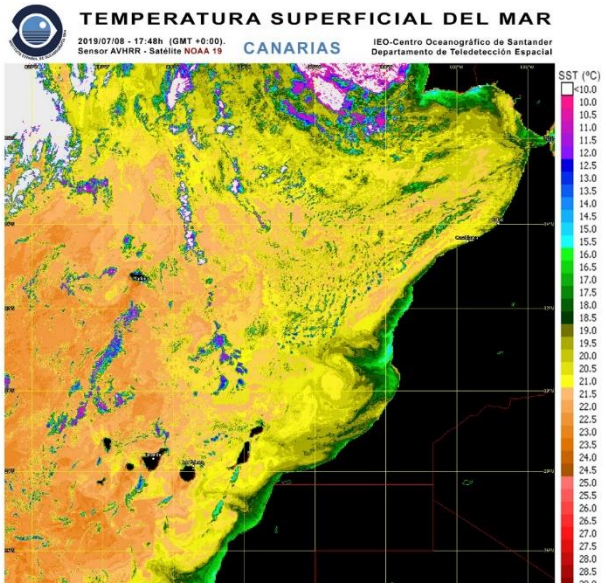


Figure 2. Satellite image of Sea Surface Temperature (SST) variation in the Canary Islands region, July 6, 2019. Source: http://www.ieo-santander.net/teledeteccion/resultados_imagenes.php, viewed the 17th April 2020.

African upwelling means the dominant way of enrichment in the region, as it brings to surface cold waters (figure 2), with high nutrients and carbon dioxide concentrations, that turns into a general increase in the primary production rates. The upwelling filaments can arrive to the islands, bringing those characteristics to the zone (*Santana-Casiano et al., 2007*).

The upwelling presents a high seasonal variability, due to changes in its driving force, the trade winds. Those winds come from northeast, and its strength reach the maximum in late-summer months (late May to beginning of September) (*Azorín-Molina et al., 2018*).

About 100 km north form Gran Canaria Island it is found the ESTOC station (European Station for Time Series in the Ocean at the Canary Islands), located at 29º10'N, 15º30'W. It was created in 1994, as a Spanish-German initiative. One of the main objectives of the station is the control of the parameters affecting the carbonate system in the Northeast Atlantic Ocean. In October 1995, oxygen, nutrient and chlorophyll concentration measurements began by the ICCM (Instituto Canario de Ciencias Marinas) and the fugacity of $CO_2$ in the atmosphere and surface water, pH and total alkalinity in the water column by the Marine Chemistry group (QUIMA), of ULPGC, in order to have knowledge of the behaviour of carbon dioxide of the area (*González-Dávila and Santana-Casiano, 2003*).

Thus, a 25-year database has been obtained, through which the seasonal and interannual evolution of carbonate system, being observed the acidification process in this period (*González-Dávila et al., 2003; González-Dávila et al., 2007; Santana-Casiano et al., 2007; González-Dávila et al.,2010; Bates et al., 2014*).

For that same purpose, it is created the oceanographic buoy Morgan 1 in 26th March 2020, in Gando, East coast of Gran Canaria Island. The buoy has different

integrated sensors, that measure fluorescence, temperature, salinity, oxygen, molar fraction and concentrations of $CO_2$ in the atmosphere and surface water and pH. It is pretended this way to improve the knowledge of carbon cycle in coastal zones due to marine acidification.

## 2. MATERIAL & METHODS

Here it is briefly summarized all the sensors integrated in the oceanographic buoy Morgan 1, from which database was obtained.

- Termosalinometer SBE 37-SI/SIP *MicroCAT*, from *Sea Bird Scientific*. It is programmed to catch temperature and salinity measurements each hour.
- $pCO_2$ Monitoring system, from *Battelle*, model 635108H1010. It measures molar fraction of carbon dioxide in seawater and atmosphere each 3 hours. These data are used to calculate partial pressure of $CO_2$, and afterwards fugacity of $CO_2$ ($fCO_2$).
- Optode 4835 Oximeter, from *Aanderaa*. Collects temperature, concentration and degree of saturation of oxygen, each 3 hours.
- $CO_2$ Flux sensor *Pro-Oceanus*, $CO_2$-Pro CV. Collects $CO_2$ partial pressure data each 3 hours.
- pH-meter *SAMI-pH*. Registers measurements of pH and temperature each 3 hours.
- Cyclops-7F Submersible fluorescence sensor, from *Turner Designs*. Measuring fluorescence each 3 hours, which is latter used to calculate chlorophyll concentration.
- *Gill MaxiMet* GMX 501 GPS Weather Station. Each hour it takes direct measures of wind speed, temperature, humidity, pressure, precipitation, solar radiation, orientation and GPS, which are later used to calculate other parameters.

Directly measured data is sent by each sensor to a central datalogger, that registers all of them and send daily by satellite signal to a server located in the ULPGC. From the original data, a treatment is done using Microsoft Excel. In addition, some calculations are made to obtain the following parameters:

a. Chlorophyll (µg/L), from fluorescence data, using the equation:

$$Chl = (Fluorescence*1.22070313)/100$$

b. Sea Surface Temperature interpolated, to get a 3-hour average, so that it can be used with the data taken each 3 hours.

c. Sea Surface Salinity interpolated, same as previous.

d. Wind speed averaged from 2 hours before and 2 hours after from meteorological station, so that extreme values, due, for example, to gusts of wind not representative of the real wind speed, are removed.

e. $CO_2$ Partial pressure in seawater, from $CO_2$ molar fraction measured by Battelle sensor, and interpolated sea surface temperature (SST) and sea surface salinity (SSS), calculated in (b) and (c). For this purpose, it is used the *Dalton (1802)* equation for partial pressure in gas mixtures:

$$P_A = X_A \,.\, P_T$$

Where $X_A$ is the molar fraction for A gas, and $P_T$ is the total pressure for the mixture. Then it is added a conversion factor to make it into atmospheres, and a correction factor for water vapour pressure, obtaining:

$$pCO_{2\ sw} = x_{CO_{2\ sw}} \cdot \frac{P.1.01325}{100} . e^{24.4543 - 67.4509 * \frac{100}{SST\ (K)} - 4.8489 . \ln\left(\frac{SST}{100}\right) - 0.000544\ .\ SSS}$$

With SST given in Kelvin degrees.

f. $CO_2$ Partial pressure in atmosphere, calculated as the previous one:

$$pCO_{2\ air} = x_{CO_{2\ air}} \cdot \frac{P.1.01325}{100} . e^{24.4543 - 67.4509 * \frac{100}{SST\ (K)} - 4.8489 . \ln\left(\frac{SST}{100}\right) - 0.000544\ .\ SSS}$$

With SST given in Kelvin degrees.

g. $CO_2$ Fugacity in seawater. To calculate the fugacity, or real pressure of $CO_2$ in seawater, virial coefficients have been used, according to the "Guide to Best Practices for Ocean CO2 Measurements" (https://www.nodc.noaa.gov/ocads/oceans/Handbook_2007.html, viewed on 28th May 2020). And so, using the following equation:

$$f_{CO_{2\ sw}} = x_{CO_{2\ sw}} p \exp\left[\left(B_{CO_{2\ sw}}(T) + 2x_{air}^2 \delta_{CO_{2\ sw}-air}(T)\right)\frac{p}{RT}\right]$$

Where, B is the virial coefficient for pure carbon dioxide gas, according to Weiss, 1974:

$$\frac{B(CO_2, T)}{cm^3 mol^{-1}} = -1636.75+12.0408\left(\frac{T}{K}\right)-3.27957 \times 10^{-2}\left(\frac{T}{K}\right)^2+3.16528 \times 10^{-5}\left(\frac{T}{K}\right)^3$$

With 265 < T/K < 320. And SST given in Kelvin degrees.

And $\delta$ is the virial coefficient for carbon dioxide in water:

$$\frac{\delta(CO_2, T)}{cm^3 mol^{-1}} = -57.7-0.118\left(\frac{T}{K}\right)$$

With 273 < T/K < 313. And SST given in Kelvin degrees.

h. $CO_2$ Fugacity in atmosphere, with the same procedure as previous one:

$$f_{CO_2\,air} = x_{CO_2\,air} p \exp\left[\left(B_{CO_2\,air}(T) + 2x_{air}^2 \delta_{CO_2\,air-air}(T)\right)\frac{p}{RT}\right]$$

With 273 < T/K < 313. And SST given in Kelvin degrees.

i. $CO_2$ Flux air-ocean, using the following equation:

$$FCO_2 = 0.24 * S * k * \Delta (fCO_{2\,sw} - fCO_{2\,air})$$

where 0.24 is a conversion factor to express data in $mmol.m^{-2}.d^{-1}$; $k = 0.251 * w^2 * (660 / Sc)^{0.5}$, which is a given gas transfer velocity, using *Wanninkhof (2014)* equation, with *w* as wind velocity ($m.s^{-1}$), Sc as Schmidt number (cinematic viscosity of seawater, divided by the gas diffusion coefficient), S as $CO_2$ solubility, and $\Delta(fCO_{2,sw} - fCO_{2,atm})$ as the difference in between $CO_2$ pressures in seawater and atmosphere. Negative values indicate that the ocean is acting as an atmospheric $CO_2$ sink.

j. $CO_2$ Fugacity at averaged temperature, with the lightly modified equation from *Takahashi et al. (2002)*, that follows:

$$(fCO_2 \text{ at } T_{mean}) = (fCO_2)_{obs} \text{ x } \exp[0.0423(T_{mean} - T_{obs})]$$

It is useful to calculate the part of the $CO_2$ fugacity oscillation which is not strictly bounded to the temperature oscillations. It is normalized to the average of SST data (20.21ºC).

k. $CO_2$ Fugacity at averaged temperature, same as previous, using the lightly modified equation from *Takahashi et al. (2002)*, that follows:

$$(fCO_2 \text{ at } T_{obs}) = (\text{Mean annual } fCO_2)_{obs} \text{ x } \exp[0.0423(T_{obs} - T_{mean})]$$

Contrary, this calculation shows the oscillation due only to the SST variation.

With the purpose of checking the accuracy of $pCO_2$ *Battelle* Monitoring System together with the $CO_2$ Flux sensor *Pro-Oceanus*, figure 3 is presented in which the similitude of the data can be seen. In addition, it has been done a *Kruskal-Wallis (1999)* variance test, which shows that there is not significant statistical difference ($P = 0.03$, exceeding the significance level, $P > \alpha$, for $\alpha = 0.05$) for measures made by both *Battelle* and *Pro-Oceanus* sensors.

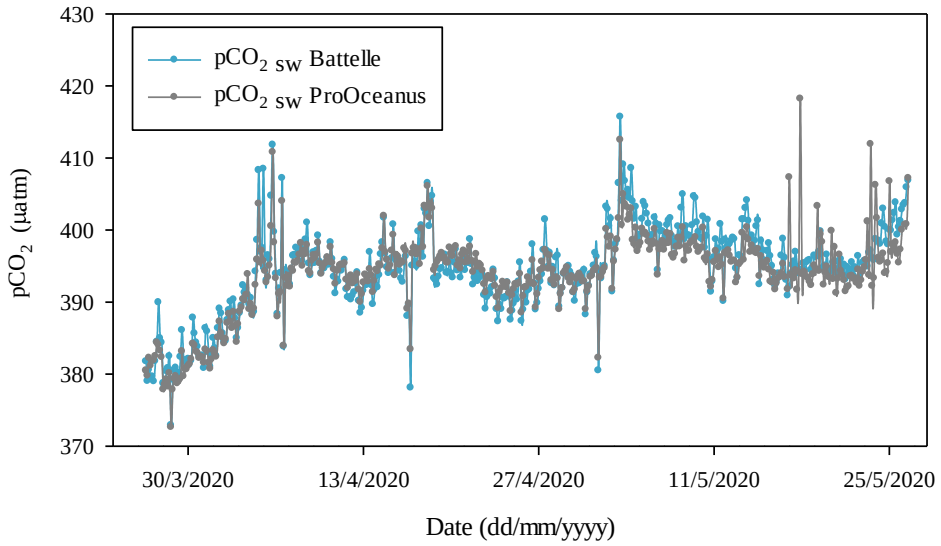


Figure 3. Time series for $CO_2$ partial pressures measured with $pCO_2$ *Battelle* Monitoring system (in blue) and $CO_2$ Flux sensor *Pro-Oceanus*.

# 3. RESULTS AND DISCUSSION

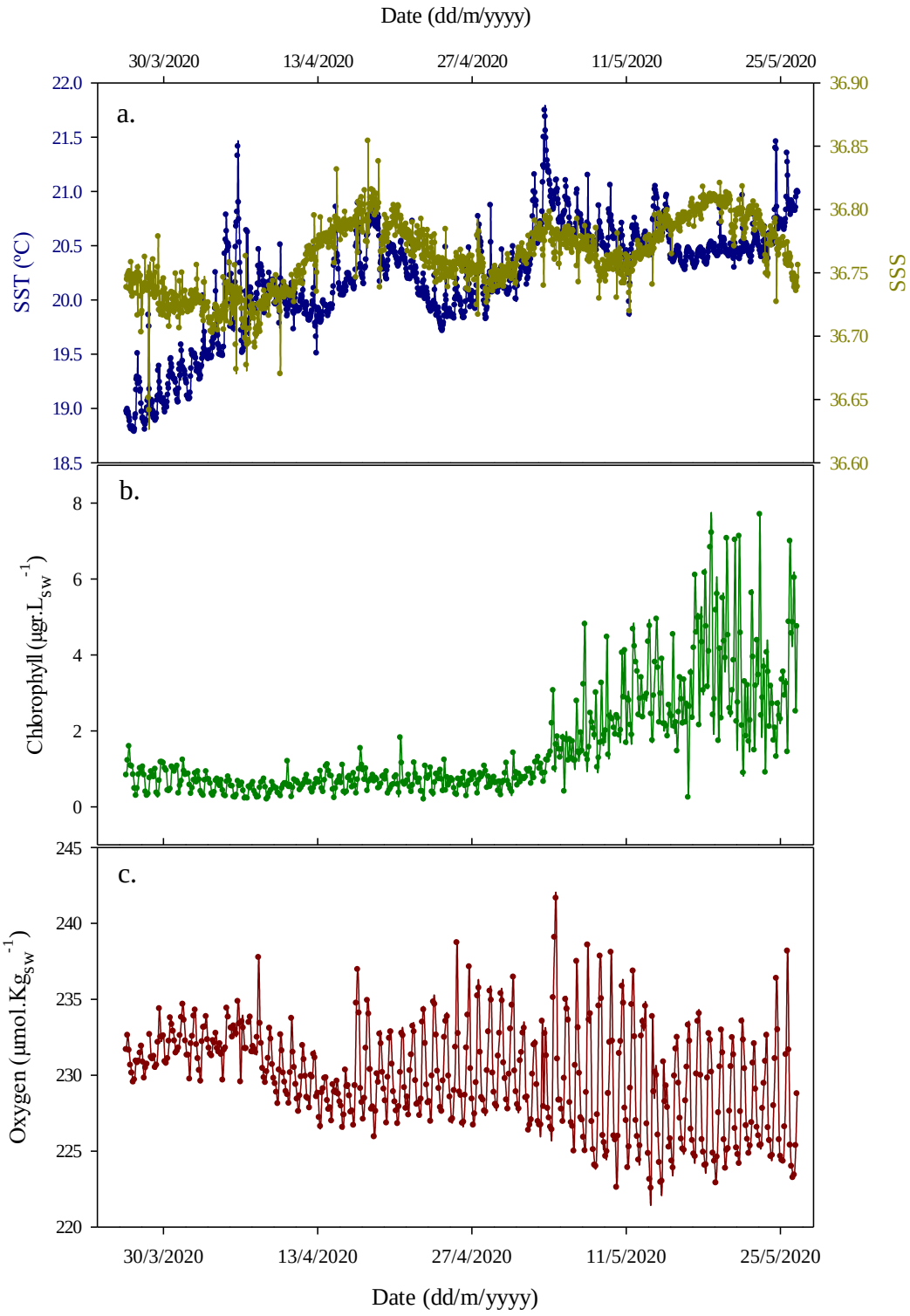


Figure 4. Plotted time series for a) SST (in ºC, blue) and SSS (yellow), b) Chlorophyll (µgr.Lsw-1) and c) Oxygen (µmol.Kgsw-1).

The SST (figure 4a, in blue) average is 20.21ºC, with extreme values of 18.79ºC as minimum, and 21.74ºC as maximum, which means that the oscillation range is 2.95ºC from late March to May. Removing extreme values and making an average of 5 first and 5 last days registered, it is seen that temperature has increased 1.61ºC, expectable result due to the beginning of spring.

Daily oscillation ranges in SST have a great variability, from days with isolation peaks, which happens in two exceptional occasions (5th April and 3th May), in which the range gets to 1.682ºC, to days with minimal oscillation, with range of 0.146ºC, probably due to cloudy days.

Attending to SSS (figure 4b, yellow), the averaged value is 36.76, with 36.85 and 36.56 as maximum and minimum registered, respectively, which means an extreme variation range 0.29. Daily oscillation ranges present peaks of variation of 0.16 and 0.011 for largest and smallest. Making an average of first and last 5 days of study, salinity has increased 0.039 during the studied period.

For the two studied months, a relatively constant fluctuation pattern appears in SST and SSS, with and approximately frequency of 28 days. With the purpose of been able to see better this phenomenon, a smoothing process was done in SST and SSS, so that strong diurnal oscillations are removed, plotted in figure 5, together with moon phases.

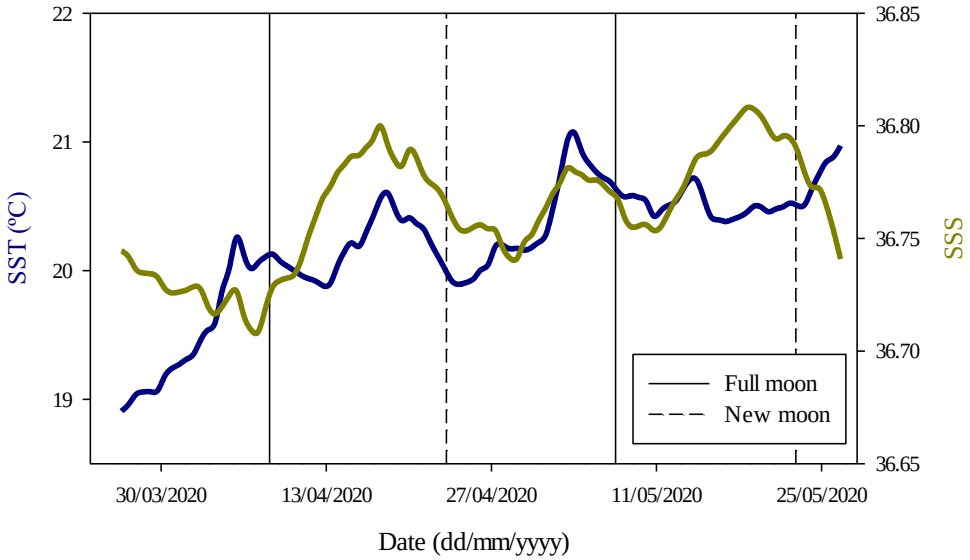


Figure 5. Time series of smoothed SST (ºC, blue) and SSS (yellow) and moon phases: full moon (solid line) and new moon (dashed line).

In new moon and full moon phases, the tides are called ‘spring tides’, and they have a bigger strength, while in between those phases, when the moon is increasing or decreasing, they are called ‘neap tides’, and they are weaker. Apparently, lower SST and SSS are found during full and new moon phases. That seems to have a relation, because

due to the spring tides in those periods, the mass water exchange with the open ocean is greater, which means that the water renovation rate is high, receiving a lower rate of isolation per $m^3$ of seawater. Contrary occurs during intermediate phases, with waning or crescent moon, when neap tides move a lower water amount, which causes a relatively greater stagnation of seawater in the bay, increasing isolation time, and SST with it. That also increases evaporation rate, which can be translated in a salinity rise, as it can be seen in figure 5, between the main moon phases.

Chlorophyll (figure 4b) presents relatively constant values from the beginning of the studied period at late March, until beginning of May, with an averaged value of 0.684 $\mu g/L_{sw}$, and an oscillation range of de 1.623 $\mu g/L_{sw}$. From the $4^{th}$ of May, higher chlorophyll concentrations are found, at the same time as daily oscillation increases, with 2.98 y 7.46 $\mu g/L_{sw}$ for the average and oscillation values, respectively. This chlorophyll increase can be explained with the increased temperature as result of the beginning of springtime5, fact naturally associated to phytoplankton blooms. Nevertheless, most of the signal was the result of the accumulation of organisms around the sensor, as it was observed by the end of May (data not shown), when the buoy was visited and cleaned with a strong reduction both in the baseline data and in the daily signal. Therefore, a cleaning protocol of the buoy has now being established.

Looking at daily oscillation, it can be seen that chlorophyll concentration decreases during the sunny hours, while they increase in a nocturnal way. As described by *Blauw et al. 2018*, oscillations of phytoplanktonic population depend on the studied timescale; oscillation produced hour-to-hour are mainly driven by physical factors as tidal currents and wind stress, that causes water sinking and vertical mixing. Following this statement, it can be deduced that observed daily oscillations can be explained by the migration of the phytoplanktonic organisms out of the shallower seawater layer to deeper waters, in hours of higher solar radiation, in order to protect from excessive isolation. That produces a drop in concentration in sunny hours.

Something similar what happens to chlorophyll occurs with oxygen concentration (figure 4c), in respect to the increase in the daily oscillation range: There are relatively small oscillations from late March, with averaged rang value of 11.2 $\mu mol.Kg_{sw}^{-1}$, that grow from mid-April, up to averaged variation of 19.12 $\mu mol.Kg_{sw}^{-1}$ until the end of the studied period. That increase in daily oscillation can be linked with the chlorophyll rise due to the phytoplankton spring bloom as, with a higher primary production rate, oxygen production in photosynthetic process is higher during the sunny hours, while in non-sunny hours the increased breathing rates produce a higher consume of $O_2$. Nevertheless, the highest daily variability is mostly due to the accumulation of organisms around the sensor, as it happened by the fluorescence sensor more than in the seawater out of the buoy influence.

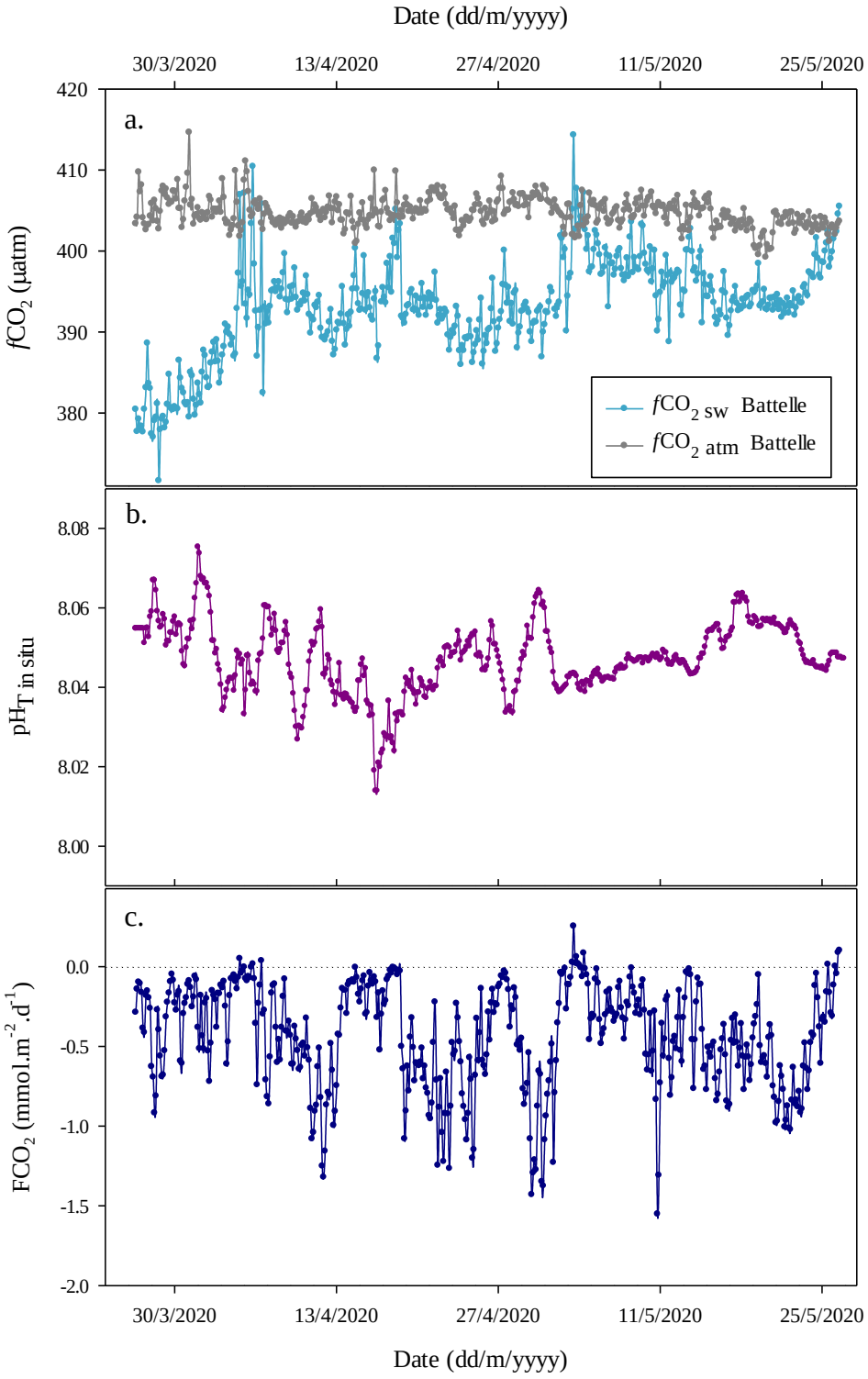


Figure 6. Plotted time series for a) $fCO_{2\ sw}$ (blue) and $fCO_{2\ atm}$ (grey), both in µatm , b) smoothed pH, and c) $CO_2$ flux (mmol.m$^{-2}$.d$^{-1}$).

Atmospheric $CO_2$ fugacity (figure 6a, grey) present quite constant values through the studied period, with an average of 404.7 µatm, and an oscillation range of 2.23 µatm. A different behaviour is seen for seawater $CO_2$ fugacity (figure 6a, blue), which shows a rate of increase, partly directly linked with the increased SST, rising from 380.46 µatm as averaged value for the first 5 days, to 397.23 µatm, for the last 5 days. That means an

increase of 16.97 µatm of carbon dioxide in marine environment. The averaged value of $fCO_2$ for the complete period of study is 393.1 µatm, with maximal and minimal peaks of 414.31 y 371.614 µatm, respectively.

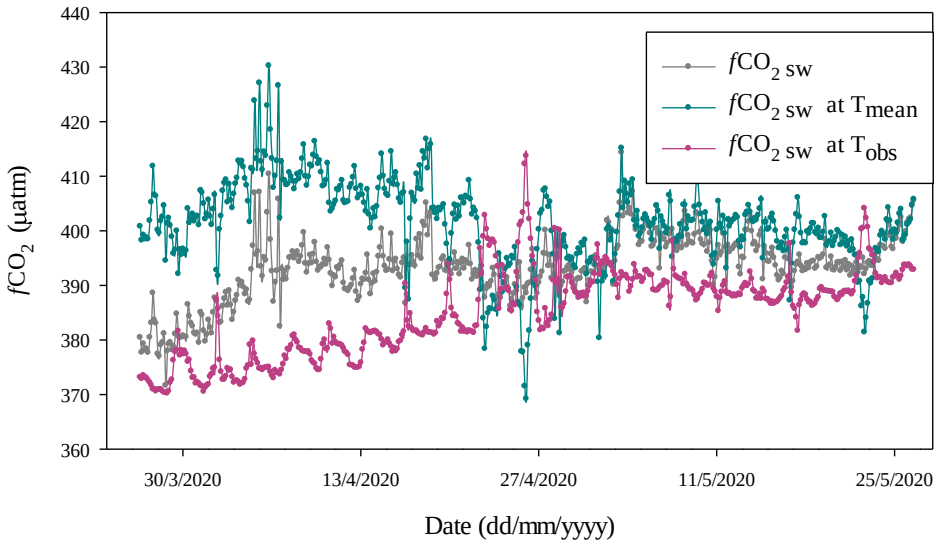


Figure 7. Time series for $fCO_{2\ obs}$ (grey), $fCO_{2\ Tmean}$ (blue) and $fCO_{2\ Tobs}$ (pink), in µatm.

Figure 7 shows plotted seawater $CO_2$ fugacity ($fCO_{2\ obs}$, grey), calculated from $CO_2$ molar fraction data obtained from $pCO_2$ Monitoring system (*Battelle*), registered in situ, together with fugacity normalized to averaged SST (20.21ºC) ($fCO_{2\ Tmean}$, blue), and fugacity calculated at observed SST ($fCO_{2\ Tobs}$, pink). $fCO_{2\ obs}$ has intermediate values between $fCO_{2\ Tobs}$ and $fCO_{2\ Tmean}$, which means that carbon dioxide concentration in Gando bay is influenced by both temperature and other processes, mainly biological activity.

The temperature rise of 1,6ºC through the two studied months, presented before, produces an increase $fCO_{2\ Tobs}$ from values of 370 to 390 ppm, approximately, which means a fugacity rise of 20 ppm, if temperature would be the only dominant factor. However, according to the calculated $fCO_{2\ obs}$ values, the oscillation is produced between 377 and 397 ppm, which denotes some biological effect in the carbon dioxide concentration, although it has smaller magnitude. From the beginning of May, it is seen a $fCO_{2\ Tmean}$ descent, which indicates the increase in biological $CO_2$ uptake, linked to the spring increase in primary production. This fact causes the three fugacities to present a more similar to each other trend.

pH has been smoothed (figure 6b) to remove extreme values, most of them related to bubbles in the tubbing. Same motive, in first days it is seen more oscillation in data, that is latter stabilized. Studied pH presents averaged values of 8.05 pH units, with a variation range of 0.34 pH units. Naturally, the water temperature increase is translated into pH decrease which value, in the observed conditions, is -0.016 pH units/ºC.

Following the SST increase shown before (1.61ºC), the corresponding pH decrease is -0.026 units. However, it also must be considered the contrary effect produced by primary production in pH, increasing it with the biological uptake of inorganic carbon. A decrease of -0.002 pH units is seen, which means that the variation due to temperature oscillation has been almost compensated by the biological effect.

In terms of the ocean-atmosphere $CO_2$ flux (figure 6c), there is a mainly negative trend, which means that ocean is acting as atmosphere $CO_2$ sink, except in some concrete moments. Averaged $FCO_2$ value is -0.4341 $mmol.m^{-2}.d^{-1}$, that is to say, -0.0191 $gr.m^{-2}.d^{-1}$, and total rate through the two studied months is -9.3234 $gr.m^{-2}$.

From that sinking rate, assuming that the $CO_2$ flux has a relatively homogeneous trend in the hole Gando bay, and that this bay presents a surface of 1665190 $m^2$ (figure 8), a budget of the $CO_2$ quantity absorbed by the bay in the studied period was done, resulting in -15.525 tons of atmospheric carbon dioxide taken by the mass of water contained in Gando bay.


Figure 8. Gando bay: Oceanographic buoy Morgan 1 as white marker, and green layer showing the bay Surface, estimated in 1.665 $km^2$.

## 4. CONCLUSIONS

Physicochemical properties registered in this study acted following the expected trend due to the arrival of springtime: There have been an increase in temperature, salinity, oxygen, chlorophyll and carbon dioxide fugacity in seawater. $fCO_2$ was mainly controlled by temperature increase and while other factors, mainly the rise in primary production rates due to springtime blooms (so it can be considered also as an indirect effect of SST rise) has a minor effect during the observed period. Both factors have opposite effects for carbon dioxide concentration trend, as the temperature increase goes

linked to the $CO_2$ increase, while a raised primary production rate means a higher $CO_2$ biological uptake, decreasing its concentration in seawater. The better correlation between the fugacity registered and the fugacity normalized at averaged temperature shows that the carbon system in Gando bay is mainly dominated by temperature oscillation whilst utilization of $CO_2$ has a minor effect.

It is been observed a relationship between SST, SSS and the moon phases. As Gando Bay is a coastal zone, relatively closed and shallow, oscillations in tide strength have a great influence in the behaviour of some of the studied parameters: In the main moon phases (full and new moon), temperature and salinity present lower values, as there is a higher renovation rate for the masses of water. However, it would be necessary a bigger database to corroborate this phenomenon.

From the obtained data, and assuming that for those two months (April and May) represent the average value along a year in this area of the Northeast Atlantic (*Santana-Casiano et al. 2007*), an annual budget is made: Total $CO_2$ flux would be 5658.76 tons.year$^{-1}$ for Gando bay, in accordance with previous studies made, that count coastal ocean as a relatively weak sink of atmospheric $CO_2$ (*Borges et al. (2005),Cai et al. (2006), Tsunogai et al. (1999))*.

However, it is necessary to keep this study with an increased database of Morgan 1 buoy to improve the knowledge of the carbonate system in this zone, at least for a year to know the seasonal variation, and for several years, to be able to observe the interannual variability.

## 5. REFERENCES

Arístegui, J., Sangrá, P., Hernández-León, S., Cantón, M., Hernández-Guerra, A. and Kerling, J.L. (1994). *Island-induced eddies in the Canary Islands.* Deep-Sea Res., vol. 41, pp. 1509– 1525.

Azorin-Molina, C., Menendez, M., McVicar, T.R., Acevedo, A., Vicente-Serrano, S.M., Cuevas, E., Minola, L. and Chen,D. (2018). *Wind speed variability over the Canary Islands, 1948-2014: focusing on trend differences at the land-ocean interface and below-above the trade wind inversion layer*. Clim. Dyn., vol. 50, pp. 4061-4081.

Bates, N.R., Astor Y.M., Church M.J., Currie K., Dore J.E., González-Dávila M., Lorenzoni L., Muller-Karger F., Olafsson J., and Santana-Casiano J.M. (2014). *A time-series view of changing ocean chemistry due to ocean uptake of anthropogenic CO2 and ocean acidification*. Oceanography, vol. 27, pp. 126–141, http://dx.doi.org/10.5670/oceanog.2014.16.

Blauw, A.N., Benincà, E., Laane, R.W.P.M., Greenwood, N. and Huisman, J. (2018). *Predictability and environmental drivers of chlorophyll fluctuations vary across different time scales and regions of the North Sea*. Prog. In Ocean., vol. 161, pp. 1-18. https://doi.org/10.1016/j.pocean.2018.01.005

Borges, A.V. (2011). *Present day carbon dioxide fluxes in the coastal ocean and possible feedbacks under global change*. Oceans and the Atmospheric Carbon Content, edited by Duarte, P. and Santana-Casiano, J.M. pp. 47-77, doi: 10.1007/978-90-481-9821-4_3.

Borges, A.V., Delille, B. and Frankignoulle, M. (2005). *Budgeting sinks and sources of $CO_2$ in the coastal ocean: Diversity of ecosystems counts*. Geophys. Res. Lett., vol. 32, L14601, doi:10.1029/2005GL023053.

Borges, A.V. and Gypens, N. (2010). *Carbonate chemistry in the coastal zone responds more strongly to eutrophication than to ocean acidification*. Limnol. Oceanogr., vol. 55, pp. 346-353.

Cai, W-J., Dai, M.H. and Wang, Y.C. (2006). *Air-sea exchange of carbon dioxide in ocean margins: A province-based synthesis*. Geophys. Res. Lett., 33:L12603. doi:10.1029/2006GL026219, www.biogeosciences.net/10/6509/2013/

Chen, C-T.A. and Borges, A.V. (2009). *Reconciling opposing views on carbon cycling in the coastal ocean: Continental shelves as sink and near-shore ecosystems as sources or atmospheric $CO_2$.* Deep-Sea Res., vol. 56, pp. 578-590.

Chen, C-T.A., Huang T-H., Chen, Y-C., Bai, Y., He, X. and Kang, Y. (2013). *Air-sea exchanges of $CO_2$ in the world's coastal seas*. Biogeosciences, vol. 10, pp. 6509-6544, doi:10.5194/bg-10-6509-2013, www.biogeosciences.net/10/6509/2013/

Frölicher, T.L., Sarmiento J.L., Paynter, D.J., Dunne, J.P., Krasting, J.P. and Winton, M. (2015). *Dominance of the Southern Ocean in anthropogenic carbon and heat uptake in CMIP5 models*. Journal of Climate, vol. 28, pp. 862-886.

Gattuso, J.P., Frankignoulle, M., and Wollast, R. (1998). *Carbon and carbonate metabolism in coastal aquatic ecosystems.* Annu. Rev. Ecol. Syst, vol. 29, pp. 405-434.

Gonzalez-Dávila, M. and Santana-Casiano, J.M. (2003). *Seasonal and interannual variability of sea-surface carbon dioxide species at the European Station for Time Series in the Ocean at the Canary Islands (ESTOC) between 1996 and 2000*. Global Biogeochem. Cycles, vol. 17(3), 1076, doi:10.1029/2002GB001993, https://www.researchgate.net/publication/237312246

Gonzalez-Dávila, M. and Santana-Casiano, J.M. (2007). *Interannual variability of the upper ocean carbon cycle in the Northeast Atlantic Ocean*. Geophysical Research Letters, vol. 34, L07608, doi: 10.1029/2006GL028145.

Gonzalez-Dávila, M., Santana-Casiano, J.M., Rueda, M.J. and Llinás, O. (2010). *The water column distribution of carbonate system variables at the ESTOC site from 1995 to 2004*. Biogeosciences, vol. 7, pp. 3067-3081, doi: 10.5194/bg-7-3067-2010, www.biogeosciences.net/7/3067/2010/

Hoffmann, L.J., Breithbarth, E., Boyd, P.W. and Hunter, K.A. (2012). *Influence of ocean warming and acidification on trace metal biogeochemistry*. Mar. Ecol. Prog. Ser., vol. 470, pp. 191-205, doi: 10.3354/meps10082.

Joos, F. and Spahni, R. (2007). *Rates of change in natural and anthropogenic radiative forcing over the past 20,000 years*. PNAS, vol. 105, pp. 1425.1430, https://doi.org/10.1073/pnas.0707386105.

Melendez, M. and Salisbury, J. (2017). *Impacts of Ocean Acidification in the Coastal and Marine Environments of Caribbean Small Island Developing States (SIDS).* Caribbean Marine Climate Change Report Card: Science Review, pp. 31–39.

Millero, F.J. (2013). *Chemical oceanography*. 4th ed. pp.259-260.

Millero, F.J., Woosley, R., Ditrolio, B. and Waters, J. (2009). *Effect of Ocean Acidification on the Speciation of Metal in Seawater*. Oceanography, vol. 22, no. 4, pp. 72-85.

Samperio-Ramos, G., Santana Casiano, J.M. and González Dávila, M. (2016). *Effect of ocean warming and acidification on the Fe(II) oxidation rate in oligotrophic and eutrophic natural waters*. Biogeochem., vol. 128, pp. 19-34., doi: 10.1007/s10533-016-0192-x.

Santana-Casiano, J. M., González-Dávila, M., Rueda, M. J., Llinás, O. and González-Dávila, E. F. (2007). *The interannual variability of oceanic $CO_2$ parameters in the northeast Atlantic subtropical gyre at the ESTOC site.* Global Biogeochemical Cycles, vol. 21(1), pp. 1–16.

Takahashi, T., Sutherland, S. C., Sweeney, C., Poisson, A., Metzl, N., Tilbrook, B., Bates, N., Wanninkhof, R., Feely, R. A., Sabine, C., Olafsson, J. and Nojiri, Y. (2002). *Global sea-air $CO_2$ flux based on climatological surface ocean $pCO_2$ seasonal biological and temperature effects*. Deep Sea Res. II, 49, pp.1601-1622.

Tsunogai S., Watanabe S. and Sato T. (1999). *Is there a "continental shelf pump" for the absorption of atmospheric $CO_2$?.* Tellus, vol. 51(B), pp. 701–712, https://doi.org/10.3402/tellusb.v51i3.16468

Wallace, R.B., Baumann, H., Grear, J.S., Aller, R.C. and Gobler, C.J. (2014). *Coastal ocean acidification: The other eutrophication problem*. Est. Coast. Shelf Science, vol. 148, pp. 1-13.

Wanninkhof, R. (2014). *Relationship between wind speed and gas exchange over the ocean revisited*. Limn. Oceanogr.: Methods, vol. 12, pp. 351-362.

# 6. PROJECT DEVELOPMENT AND PERSONAL VALORATION

## 6.1. Detailed description of the activities developed through the TFT realization

The realization of the TFT has involved the following activities:

- Preparation and launch of the oceanographic buoy MORGAN I, subproject CanOA from project CanBIO, financed by Canarian government and Loro Parque foundation.
- Data treatment with program Microsoft Excel, to create a 2-months database of all the sensors integrated in the buoy.
- Plotting the database to show the most relevant considered data for this study.
- Bibliographic review of marine acidification, biogeochemical cycles and other themes related.
- Writing of the present work joining the researched bibliography and the results obtained with the database.
- Face meetings and videoconferences with tutors.

## 6.2. Received formation

The received formation includes detailed descriptions of the sensors integrated in the oceanographic buoy; theorical aspects about the atmosphere-ocean carbonate system; Microsoft Excel program notions for the treatment of data received, including Macro use; explanations about the creation of a bibliography review appropriate to the subject of study.

## 6.3. Integration and implication level within the department and relations with the personnel

Mainly by my tutors, Melchor and Magdalena, and by Adrián Castro Álamo, associate research technician, but also by other members of the QUIMA group, and external collaborators of this project, both in the research field and informatic and environmental consulting professionals , the degree of welcome I have received has been absolute, attending to all of the doubts and suggestions that I have been able to contribute during the process, and maintaining all the time a cordial and close relationship, which has made my stay, though brief, very satisfactory.

## 6.4. Most significant positive and negative aspects related to the TFT development

The positive aspects include the fact of have been able to collaborate in the launch of an oceanographic buoy, a not so common or easy to achieve event; the possibility of working with people who have shown a perfect collaboration with my work, helping me in everything I have needed, and contributing a great deal of new knowledge.

As negative part, the impediment to complete all the planned activities for these practices, produced by the health emergency situation caused by Coronavirus-19. For this reason, the programmed activities have been replaced by new ones, adapted to the current situation, such as tutoring via email and videoconferences, in addition to weekly progress reports, which have been delivered every Monday.

## 6.5. Personal assessment of the learning achieved throughout the TFT

This project has greatly improved my knowledge of the covered topic, the development of bibliographic reviews and informatic skills in terms of programming and data processing. This will allow me to adapt to new similar situations, such as the continuation of academical training, or future research work.